Nonlinear Attenuation Factor Based Rat Swarm Optimization Algorithm on Off-grid Renewable Energy System

Xun Liu, Jie-Sheng Wang*, Song-Bo Zhang, Yuan-Zheng Gao, Jia-Hui Zhao

Abstract—**To address the optimization modeling and economic cost issues of microgrids in specific regions, this paper proposes an improved rat swarm optimization (RSO) algorithm to solve the optimization problem of off-grid hybrid renewable energy systems. In response to the low optimization efficiency, insufficient stability and premature convergence issues in the traditional RSO algorithm during the path planning process, this paper introduces six nonlinear attenuation factors, including cubic attenuation factor, cube root attenuation factor, exponential-binomial distribution attenuation factor, logarithmic attenuation factor, sine attenuation factor and cosine attenuation factor, which are respectively used as global search factors to regulate the convergence speed and distribution characteristics of the search strategy, thereby enhancing the algorithm's search capability within the feasible domain. The optimized algorithm is applied to the optimal design of hybrid renewable energy systems. Experimental results show that in the three case studies, the system with nickel-iron batteries performs best, with a minimum life cycle cost of $1,015,118 and an energy cost reduced to $0.2134/kWh, significantly improving the economic and feasibility of the system.**

Index Terms—**renewable energy system, microgrid, rat swarm optimization algorithm, Nonlinear factor**

I. Introduction

With the rapid evolution of the global energy market, the focus on sustainable and environmentally friendly energy sources has been increasing. Although various renewable energy sources have become important alternatives, their inherent intermittency still poses reliability challenges for scholars around the world. To address this issue, hybrid energy systems integrating multiple renewable energy sources and energy storage technologies have been widely studied and are regarded as an effective solution [1].

This study examines a combination of renewable energy sources that is mostly utilized for producing electricity in remote locations; It may be thought of as an off-grid microgrid. Common methods in this field can be roughly classified into three categories. The first category is the analysis method based on simulation software. Sinha et al. systematically introduced 19 simulation tools commonly used in the design of hybrid energy systems in Ref. [2], such as HOMER and HYBRID 2. However, this type of method is relatively limited in the selection of system components, and users find it difficult to intuitively match the optimal configuration. Moreover, it is impossible to directly access the specific details of the calculation process or the optimization algorithm. The second category is deterministic methods, including traditional mathematical methods such as probability analysis [3]. Although these methods can provide high accuracy in specific scenarios, their solution performance is strongly related to the complexity of the microgrid problem and they are prone to getting stuck in local optima. The third category is meta-heuristic algorithms, which are considered the most promising optimization methods at present. This method regards the optimization problem as a black box, relying only on input and output, without the need to calculate the gradient of the search space, thereby effectively avoiding local optima through a gradient-free mechanism. However, according to the No-Free-Lunch theorem, no algorithm can maintain optimal performance in all optimization problems. A specific meta-heuristic algorithm may perform well in a certain type of problem but be inefficient in others. To increase the solution capacity of microgrid scale optimization, this research suggests an enhanced rat swarm optimization technique.

Researchers have established various renewable energy systems using different methods so that these systems can be applied to a wider range of regions. Different configurations of renewable energy are outlined in various literatures, which can be either single-source systems or hybrid systems [4]. They can be composed of photovoltaic panels [5], wind turbines, etc. [6-8] or renewable energy systems with multiple mixed energy sources. Marocco et al. developed the cost-emission Pareto front of different HRES configurations by using the particle swarm optimization algorithm to study systems including photovoltaic panels, wind turbines, batteries, hydrogen-based systems and diesel generators, with the levelized cost of electricity (*LCOE*) as the objective function, to better understand the potential of

Manuscript received February 21, 2025; revised April 18, 2025. This work was supported by the Basic Scientific Research Project of Institution of Higher Learning of Liaoning Province (Grant No. LJ222410146054), and Postgraduate Education Reform Project of Liaoning Province (Grant No. LNYJG2022137).

Xun Liu is a postgraduate student at School of Electronic and Information Engineering, University of Science and Technology Liaoning, Anshan, 114051, P. R. China (e-mail: lx@stu.ustl.edu.cn).

Jie-Sheng Wang is a professor of School of Electronic and Information Engineering, University of Science and Technology Liaoning, Anshan, 114051, P. R. China (Corresponding author, phone: 86-0412-2538246; fax: 86-0412-2538244; e-mail: wjs@ustl.edu.cn).

Song-Bo Zhang is a postgraduate student at School of Electronic and Information Engineering, University of Science and Technology Liaoning, Anshan, 114051, P. R. China (e-mail: zsb@stu.ustl.edu.cn).

Yuan-Zheng Gao is a postgraduate student at School of Electronic and Information Engineering, University of Science and Technology Liaoning, Anshan 114051, China (E-mail: gyz@stu.ustl.edu.cn).

Jia-Hui Zhao is a postgraduate student at School of Electronic and Information Engineering, University of Science and Technology Liaoning, Anshan, 114051, P. R. China (e-mail: zjh@stu.ustl.edu.cn).

renewable energy-based systems in off-grid applications [9]. The hybrid system established by Nallolla is composed of solar photovoltaic systems, wind turbines, diesel generators, battery storage systems, converters, electrolyzers and hydrogen storage tanks to provide uninterrupted power and meet the different load demands of different communities in the village of Chittoor Doddipalli, Andhra Pradesh, India. Then, the HOMER software was used to optimize and conduct technical and economic analysis of this system [10]. The technologies included in the system designed by Viole are photovoltaic, concentrated solar power, diesel generators, batteries, and hydrogen storage, etc. The power system optimization model was applied to this case study to predict energy demand, cost assumptions for 2030 and capacity factors for specific sites [11]. Ayodele et al. explored an off-grid renewable energy system composed of solar photovoltaic and wind turbines, with a hydrogen storage scheme by using the particle swarm algorithm for optimal sizing planning and control to meet the electricity demand of a clinic [12]. Arabzadeh et al. investigated the integration of a large amount of wind and solar power generation capacity into Luxembourg's energy framework to address challenges such as variability, intermittency, and wind curtailment. It delved into scenarios including power-to-heat and vertical agriculture technologies to enhance system flexibility and promote the integration of renewable energy [13].

Nonlinear factors, as one of the important strategies for improving optimization algorithms, play a key role in enhancing algorithm performance and have been widely studied by scholars at home and abroad. Sun et al. designed a nonlinear decreasing strategy related to the exponential function to replace the linear convergence factor, enabling the improved whale optimization algorithm to effectively avoid local optimal solutions [14]. Li et al. used a set of nonlinear scaling factor functions to improve the genetic algorithm and proved that it could make accurate performance predictions for engines under a wide range of conditions [15]. Zhang et al. introduced nonlinear adaptive weights to improve the whale algorithm, allowing search agents to adaptively explore the search space and balance the exploration and exploitation phases [16]. Majumdar et al. used nonlinear adaptive weight factors to adaptively explore the search space to improve the honey badger optimization algorithm [17]. Zhang M et al. used a nonlinear control parameter strategy based on the sine function and a nonlinear control parameter combination strategy to improve the grey wolf algorithm, which was verified on benchmark functions [18].

The hybrid renewable energy system adopted in this paper is based on the regional data of a certain area in India provided by Ref. [19], including hourly solar radiation, environmental temperature, wind speed, and needs for water throughout year. The structure includes a diesel generator, solar power generation, wind turbines, biomass electricity generation, a diesel generator, battery packs (lead-acid batteries, lithium batteries and nickel-iron batteries), and reciprocal converters to supply power to local residents and support the operation of reverse osmosis seawater desalination systems. Compared with Ref. [19], in order to improve system stability and lessen the impact of variations in renewable energy, this study also incorporates wind energy and diesel generators. Residents' demand-side data is cited in Ref. [20], which proposes three demand-side management schemes: low-cost high-power rated appliances (HPRALC), medium-cost medium-power rated appliances (MPRAMC) and high-cost low-power rated appliances (LPRAHC). This paper selects the HPRALC scenario, mainly based on two considerations: first, this type of appliance is relatively common in the local area; second, this paper focuses on optimizing the hybrid renewable energy system and energy management strategies to reduce life cycle costs, while Ref. [20] mainly studies the impact of demand-side management schemes on costs and does not involve the algorithm optimization part.

To sum up, this paper's significant innovations are listed here. In the rat swarm optimization algorithm, six nonlinear decay factors, including cubic decay factor, cube root decay factor, exponential-binomial distribution decay factor, logarithmic decay factor, sine decay factor and cosine decay factor, are respectively used as global search factors to regulate the convergence speed and distribution characteristics of the search strategy, thereby enhancing the algorithm's search capability within the feasible domain. Additionally, it is used to address the optimization issue with renewable energy systems.

The overall structure of this paper is as follows. Section II introduces the components of the hybrid renewable energy system and the related objective functions. Section III explains the rat swarm optimization algorithm and the proposed improved method. Section IV validates the improved algorithm in test functions. Section V applies the improved algorithm to an engineerin background, verifies three cases using the improved rat swarm algorithm SIRSO, and compares it with other algorithms. Section VI summarizes the full text and presents prospects.

II. Mathematical Modeling of the System and Objective Function

In the simulation of off-grid green power systems, we usually start from four core aspects. Firstly, from the perspective of energy sources, we consider the uncertainty and volatility of renewable energy and build a reasonable energy supply model. The types of renewable energy in this paper include solar energy [21], wind energy [22] and biomass energy [23]. To enhance the stability of the system, a diesel generator is added on this basis to improve system stability. Secondly, from the perspective of energy load, we analyze the demand characteristics of different load types. The energy load in this paper can be divided into residential demand-side load and seawater desalination device load [24-26], the former is for the daily life needs of residents, and the specific data can be found in reference [20], while the latter is to provide the required electricity for the seawater desalination device, and the specific data can be found in Ref. [29], in order to ensure its normal operation to provide fresh water for residents. Next, from the standpoint of storing electricity, we investigate how devices for storing energy help balance the supply and demand for energy and create a model of energy storage that is both inexpensive and efficient. This paper mainly adopts three types of batteries, namely lead-acid batteries, lithium-ion

batteries and nickel-iron batteries [29]. Finally, from the perspective of energy management, we propose a scheduling and management strategy based on optimization algorithms to achieve the rational allocation and efficient operation of various resources.

A. Diesel Generator System

For the specific types of solar energy, wind energy and biomass energy adopted and the modeling formulas, please refer to Ref. [29]. The newly added diesel generator serves as a continuous power supply unit [27], with its rated power set at 50 kW [21]. The hourly fuel consumption of the DG (F_{DG}) can be obtained by:

$$F_{DG}(t) = (a_{DG} \times P_{DG,gen}(t) + b_{DG} \times P_{DG,rat}) \ l/h \quad (1)$$

The coefficients of the DG usage curve in Eq. (1) are denoted by the numbers a_{DG}=0.246(l/kWh) and b_{DG}=0.08145(l/kWh). The generated power and rated power of DG are denoted by $P_{DG,gen}(t)$ and $P_{DG,rat}(t)$, respectively. The diesel generator sets yearly total fuel consumption may be computed in liters as follows:

$$TYFCIL = \sum_{t=1}^{8760} F_{DG}(t) \quad (2)$$

Based on the hourly fuel consumption, the estimated hourly carbon dioxide emissions of the DG is described as follows [28].

$$CO_2 = SE_{CO_2}(kg/l) \times F_{DG}(t)(l/h) \quad (3)$$

where, SE_{CO2} represents the carbon dioxide emission ratio per liter of diesel, with a value of 2.7 kilograms per liter. The estimated total annual carbon dioxide emissions of DG is defined as:

$$TY_{CO_2}emission = \sum_{t=1}^{8760} CO_2(t) \quad (4)$$

B. Energy Management Strategies

In the energy management strategy of this system, the coordinated control process is divided into six operation modes. Based on the Ref. [29], mode 5 and mode 6 have been added due to the introduction of diesel generators. The specific schematic diagram is shown in Fig. 1.

(1) Mode 1. Under this operating mode, the system achieves a balance between power supply and demand, with the net energy generated being zero. Therefore, the battery pack's energy stays constant.

(2) Mode 2. Under the mode, renewable power resources first meet the load demand, and then the excess energy generated is stored in the battery. At this time, the battery's power is between its maximum and minimum storage limits. To supply energy is to the load.

(3) Mode 3. The excess energy is transferred to the dumping load after the battery has reached its maximum capacity and the renewable energy sources have met the load requirement. The transmitted power is referred to as E_{dump}.

(4) Mode 4. The battery fills the energy gap in this mode of operation when the energy produced by renewable energy sources is less than the load requirement. E_{dch} stands for energy discharged from the battery.

(5) Mode 5. The diesel generator set will run at its rated power to satisfy the load requirement and charge the battery pack if the energy produced by renewable energy sources and batteries is not enough to meet the demand for load. The DG shuts off when the renewable energy begins to provide enough power to fulfill the entire load need.

(6) Mode 6. The battery's internal power is depleted in this operating mode because the energy from renewable sources is less than the necessary load demand. At this point, a gap occurs, and the program outputs NAN.

C. Objective Function: Life Cycle Cost

The objective function of this paper adopts life cycle cost. The cost composition of solar power generation, wind power generation and biomass power generation components can be found in Ref. [29]. The load loss rate ($LPSP$) is used as the reliability evaluation index, where $LPSP$ is the percentage of the total load loss to the total demand load.

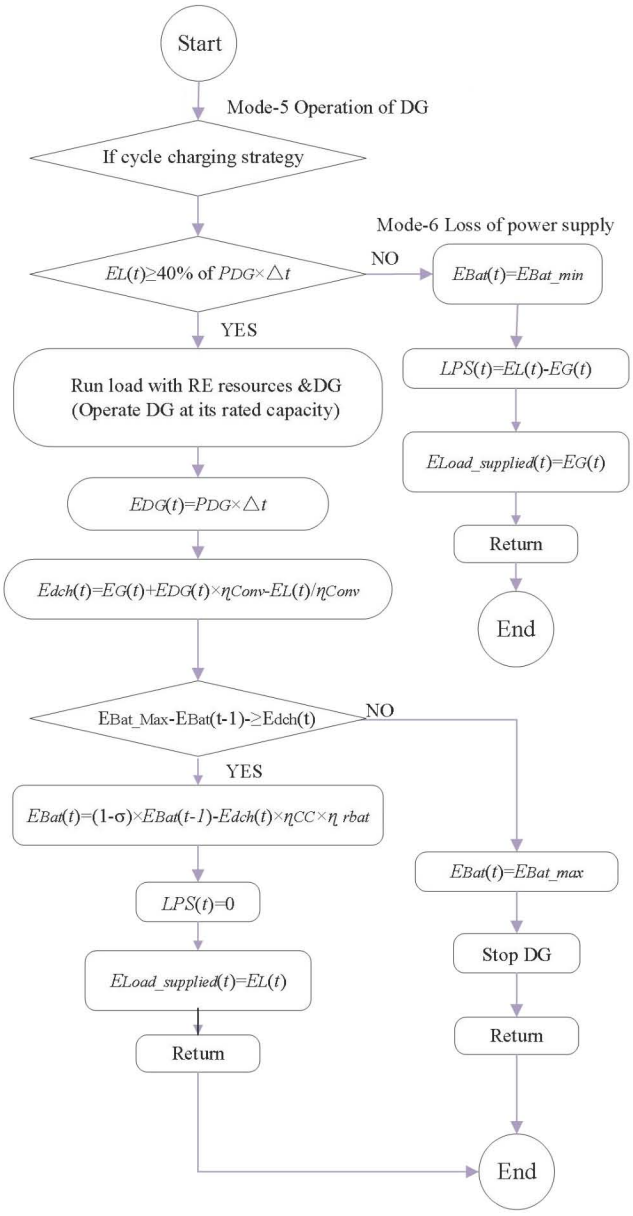

Fig. 1 Flowcharts of Mode 5 and Mode 6.

$$LCC(N_{PV},N_{WT},N_{BAT}) = \sum_{PV,WT,BMG,DG,BAT,ROD,BDC-CC}^{min} (LCC) \quad (5)$$

where, N_{PV},N_{WT},N_{BAT} are the independent variables of the system, representing thenquantities of solar power plants, wind turbines, and batteries. The composition of *LCC* is defind as follows:

$$LCC=ICC+EREC+P_{O\&M}+P_{REP}+P_{FUEL} \quad (6)$$

where, *ICC* represents the initial capital cost, *EREC* represents the installation cost, $P_{O\&M}$ represents the operation and maintenance cost, P_{REP} represents the replacement cost and P_{FUEL} represents the current value of the fuel cost.

(1) Life cycle cost of diesel generator system

Diesel generators are typically composed of a diesel engine and a generator (usually an alternator). Their life cycle costs consist of five parts: initial cost, installation cost, replacement cost, operation and maintenance cost, and fuel cost.

$$\begin{aligned} LCC_{DG} &= ICC+EREC+P_{O\&M}+P_{REP}+P_{FUEL} \\ &= \left(C_{DG,cap}\right)+\left(C_{DG,erect}\times\sum_{p=1}^{N_r}\frac{(1+x)^{pN_C-1}}{(1+y)^{pN_C-1}}\right)+\left(C_{DG,YOM})\times\sum_{i=1}^{N}\frac{(1+x)^{i-1}}{(1+y)^i}\right) \\ &+\left(C_{DG,rep}\times\sum_{p=1}^{N_r}\frac{(1+x)^{pN_C-1}}{(1+y)^{pN_C}}\right)+\left(TAFCIL_{DG}\times\sum_{i=1}^{N}\frac{(1+x)^{i-1}}{(1+y)^i}\right) \end{aligned} \quad (7)$$

where, $TAFCIL_{DG}$ is the entire amount of fuel consumed in liters per year, $C_{DG,cap}$ is the initial cost of the diesel generator, $C_{DG,erect}$ is the installation cost each time, $C_{DG,YOM}$ is the cost of keeping it running during the life of the system, as well as $C_{DG,rep}$ is the price of reset each time.

D. Energy Cost

The energy cost (*COE*) is calculated through *LCC* (*Life Cycle Cost*), with the unit of dollars per kilowatt-hour. *COE* is one of the most commonly used indicators when evaluating the economic benefits of Hybrid Renewable Energy Systems (HRES). Its calculation is realized by:

$$COE(\$/kWh) = \left(\frac{LCC}{\sum_{t=1}^{8760}E_L(t)}\right)\times CRF \quad (8)$$

where, *CRF* is the capital recovery factor, and its calculation formula is difined as:

$$CRF = \frac{y\times(1+y)^N}{(1+y)^N-1} \quad (9)$$

where, *y* denotes the paper interest rate and *N* denotes the project's duration.

E. Constraint Conditions

The constraints of this paper mainly include four aspects: solar panels, wind turbines, batteries and diesel generators. The first three have been described in Ref. [29]. Under high load conditions, diesel generators (DG) have higher efficiency [30]. As a result, 40% of the diesel generator's rated capacity is the minimum load required for operation. That is, the operation of diesel generators needs to follow the following restrictions [19].

$$\frac{E_L(t)}{\eta_{Conv}} \geq 40\%\ P_{DG}\times\Delta t \quad (10)$$

where, the hourly demand for electricity is represented by $E_L(t)$, the bidirectional converter's effectiveness by η_{Conv}, the diesel generator's rated output by P_{DG}, and the operational time period by Δt.

III. Rat Swarm Optimization Algorithm Based on Nonlinear Attenuation Factor

A. Rat Swarm Optimization Algorithm

Rat swarm optimization algorithm [31] is a meta-heuristic optimization algorithm, which is inspired by the hunting behavior of rats in nature. The optimization process of this algorithm mainly consists of two core stages: prey tracking and prey capture.

(1) Prey fracking

When the prey is discovered by the nearest individual in the population (the current optimal individual), the remaining individuals will dynamically adjust their movement trajectories based on their current positions and gradually approach the optimal individual. This process is driven by a group collaborative competition mechanism, enabling each individual mouse to continuously optimize its position within the search space to enhance global search efficiency and improve the optimization ability. The position update formula for this prey tracking mechanism is as follows:

$$P_V = A\times X_{i,t}+C\left(X_{best}-X_{i,t}\right) \quad (11)$$

where, P_v represents the updated position of the rat, $X_{i,t}$ defines the current position of the *i*-th rat in the *t*-th generation, and X_{best} is the global optimal position. The calculation formulas for *A* and *C* are as follows:

$$A = R-t\times R/t_{\max} \quad (12)$$

$$C = 2\times rand(0,1) \quad (13)$$

Let *t* be the current iteration count and t_{max} be the maximum iteration count. Therefore, *R* and *C* are random numbers within the intervals [1, 5] and [0, 2], respectively.

(2) Prey capture

After the group of mice approaches the prey, individuals seek the optimal attack point by constantly updating their positions to capture the prey more effectively. This process ensures that the mice can quickly approach and ultimately capture the prey in a dynamically changing environment through continuous adjustment of positions, thereby achieving the optimization goal. The mathematical model of this attack behavior can be specifically described by the following equation.

$$P_i(t+1) = \left|X_{best}-P_V\right| \quad (14)$$

where, P_i (t+1) represents the position of the i-th mouse at the (t+1)-th time.

B. Rat Swarm Optimization Algorithm Based on Nonlinear Attenuation Factor

In the original rat swarm algorithm, the linearly decreasing method of parameter A significantly affects the capacity to search globally. Due to the lack of sufficient adaptive coordination ability in the decreasing process of the global search factor A, this limits the algorithm's effective exploration and global optimization in complex solution spaces. To address this issue, this paper proposes an improvement to parameter A by adopting six different nonlinear attenuation factors. Specifically, the improved attenuation factors include: cubic attenuation factor, cube root attenuation factor, exponential-binomial distribution attenuation factor, logarithmic attenuation factor, sine attenuation factor, and cosine attenuation factor.

Each attenuation factor dynamically adjusts the parameter A according to its specific mathematical form, thereby enhancing the algorithm's adaptability at different search stages. The cubic attenuation factor causes A to decrease rapidly at first, then gradually, and then rapidly again. The cube root function makes A decrease rapidly in the middle of the iteration count. The exponential-binomial distribution factor oscillates and attenuates A slowly at the beginning, rapidly in the middle, and then gradually. The logarithmic attenuation factor causes A to decrease rapidly at first and then gradually. The sine attenuation factor uniformly oscillates and attenuates A globally. The cosine attenuation factor causes A to decrease gradually at first and then rapidly. The specific improved formulas and attenuation curves are shown in Table I and Fig. 2. The introduction of these nonlinear attenuation factors enables the rat swarm algorithm to fully explore a broader solution space and effectively improves the convergence speed of the algorithm, especially demonstrating stronger global search ability and higher solution quality in complex optimization problems.

IV. Simulation Experiment and Result Analysis of Test Function

The CEC2022 optimization function test set is a commonly used benchmark test function set. This test set includes 12 single-objective functions, among which F1 is a classic unimodal function, F2-F5 are multimodal functions with multiple local extremum points, aiming to examine the global search ability of the algorithm in complex solution spaces. F6-F8 are composite functions that mix the properties of numerous optimization problems to evaluate the algorithm's adaptability and resilience across diverse contexts. F9-F12 are composite functions with varying weights and bias values, which complicates the technique's optimization process and necessitates the algorithm's ability to tackle multilevel and multidimensional situations.

To verify the effectiveness of the improved algorithm, this experiment utilized the CEC2022 optimization function test set. In the experiment, each function was tested with 500 iterations and a population size of 50, and the average value was taken from 30 independent experiments to ensure the statistical reliability of the experimental results. The simulation process was divided into two stages: Firstly, the first part verified the reliability of the nonlinear attenuation factor. Secondly, through comparative analysis with other optimization algorithms, the experimental results fully demonstrated the advantages of the proposed improved algorithm in terms of solution efficiency and accuracy, showing strong global search ability and faster convergence speed, thereby verifying the effectiveness and adaptability of the improved algorithm in complex optimization problems.

To verify the effectiveness of the improved algorithm, this experiment utilized the CEC2022 optimization function test set. In the experiment, each function was tested with 500 iterations and a population size of 50, and the average value was taken from 30 independent experiments to ensure the statistical reliability of the experimental results. The simulation process was divided into two stages: Firstly, the first part verified the reliability of the nonlinear attenuation factor. Secondly, through comparative analysis with other optimization algorithms, the experimental results fully demonstrated the advantages of the proposed improved algorithm in terms of solution efficiency and accuracy, showing strong global search ability and faster convergence speed, thereby verifying the effectiveness and adaptability of the improved algorithm in complex optimization problems.

Table I. The formula of the improved attenuation factor A

Number	Decay factor	Improved algorithm name	Parameter equation
1	Cubic attenuation factor	CURSO	$A_1 = r \times (-[(2 \times \frac{t}{t_{\max}} - 1)^3 + 1] \times 2.5$
2	Cubic root attenuation factor	RORSO	$A_2 = r(-[\sqrt[3]{2 \times \frac{t}{t_{\max}} - 1} + 1] \times 2.5$
3	Exponential-binomial distribution attenuation factor	EXRSO	$A_3 = 4 / (1 + e^{20 \times t/t_{\max}}) + binornd(1,\ 0.5)$
4	Logarithmic attenuation factor	LORSO	$A_4 = r \times \log(t / t_{\max}) \div \log(1/2.1) \times \frac{7}{9}$
5	Sinusoidal attenuation factor	SIRSO	$A_5 = r \times (2 \times \sin(\frac{-\pi}{2} \times \frac{t}{t_{\max}}) + 2) \times 2.5$
6	Cosine attenuation factor	CORSO	$A_6 = r \times \cos(\frac{\pi}{2} \times \frac{t}{t_{\max}}) \times 2.5$

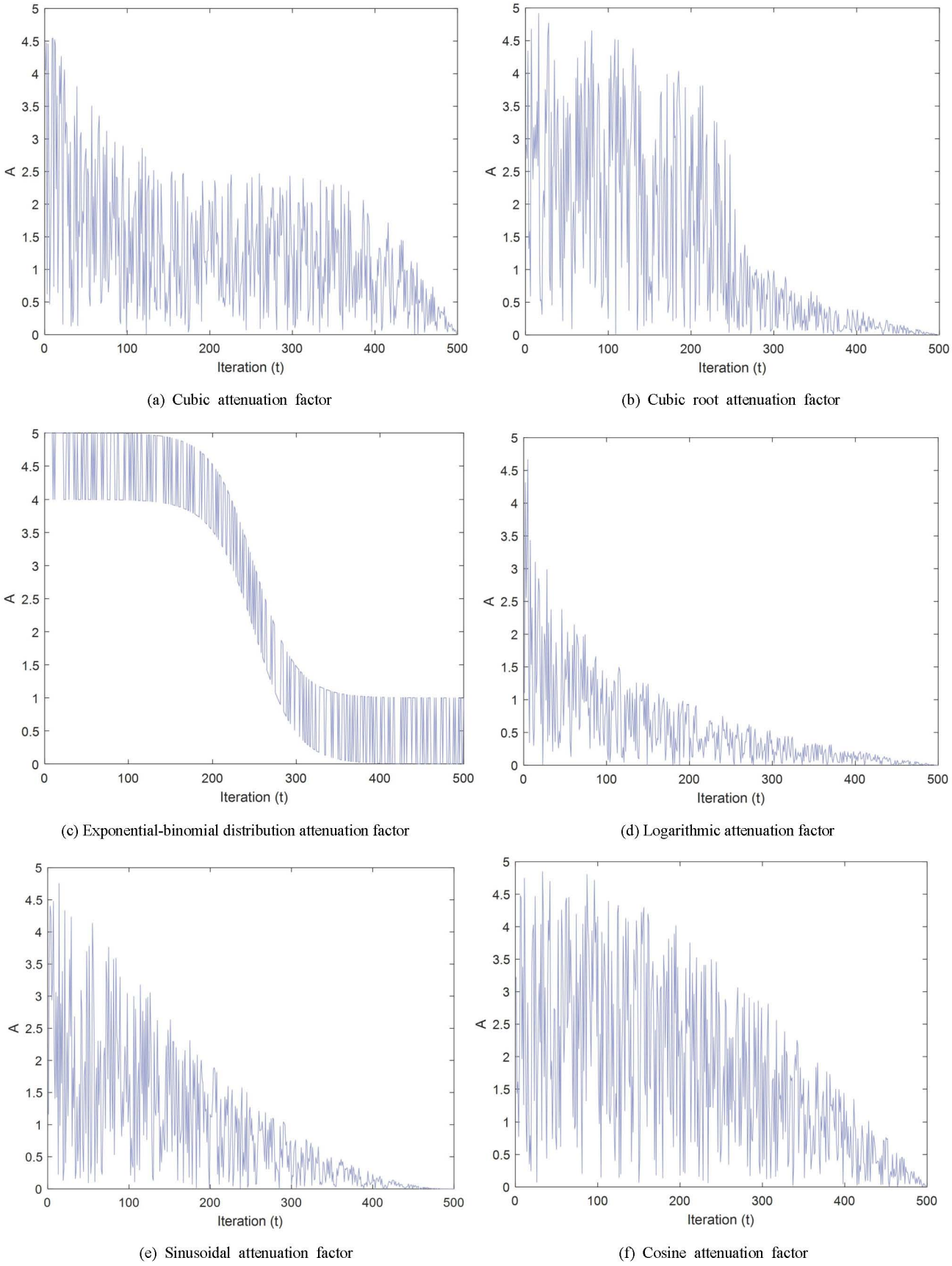

(a) Cubic attenuation factor

(b) Cubic root attenuation factor

(c) Exponential-binomial distribution attenuation factor

(d) Logarithmic attenuation factor

(e) Sinusoidal attenuation factor

(f) Cosine attenuation factor

Fig. 2 Different images of nonlinear attenuation factor *A*.

A. Rat Swarm Optimization Algorithm Based on Nonlinear Attenuation Factors

It can be seen from Fig. 3 that each nonlinear attenuation factor has improved the performance of the rat swarm optimization algorithm. Among them, SIRSO performed the best, achieving the minimum average value in 8 test functions, namely F1, F4, F5, F6, F7, F8, F10 and F12. CURSO ranked second, achieving the minimum average value in 4 test functions, namely F2, F3, F9 and F11. The specific values are shown in Table II. The average value of

SIRSO in functions such as F1, F4, F5 and F6 is significantly lower than that of other algorithms, especially in F6, where its best value is 3.946E+03, far lower than the optimal values of other algorithms. This indicates that SIRSO can better handle complex optimization problems with boundary constraints.

By comparing the standard deviations of various algorithms, it can be observed that SIRSO not only has an advantage in the average value but also has smaller volatility, indicating its higher stability. The standard deviations of other algorithms are generally larger, especially in complex problems such as F6 and F9, where the search processes of other decay factors are less stable than that of SIRSO. The improved rat swarm optimization algorithm, particularly SIRSO, by introducing a nonlinear decay factor, not only improves the convergence speed but also enhances its adaptability and robustness in various complex optimization problems.

TABLE II. SIMULATION RESULTS OF THE TEST FUNCTION

Function	Meteic	RSO	CURSO	RORSO	LORSO	CORSO	SIRSO	EXRSO
	Ave	2.961E+03	2.103E+03	2.184E+03	9.870E+05	2.706E+03	**1.934E+03**	4.378E+03
F1	Std	1.576E+03	5.470E+02	9.820E+02	4.518E+06	9.468E+02	3.923E+01	1.764E+03
	Best	1.617E+03	9.922E+02	1.017E+03	1.351E+04	1.776E+03	1.815E+03	1.605E+03
	Ave	7.591E+02	**7.089E+02**	7.502E+02	2.464E+03	8.209E+02	7.310E+02	9.168E+02
F2	Std	2.125E+02	1.027E+02	1.265E+02	7.969E+02	2.245E+02	1.338E+02	2.592E+02
	Best	5.097E+02	5.295E+02	5.023E+02	1.256E+03	5.355E+02	5.088E+02	5.046E+02
	Ave	6.422E+02	**6.376E+02**	6.422E+02	6.900E+02	6.435E+02	6.395E+02	6.455E+02
F3	Std	6.630E+00	5.458E+00	6.321E+00	1.299E+01	5.908E+00	5.133E+00	6.655E+00
	Best	6.317E+02	6.259E+02	6.291E+02	6.678E+02	6.318E+02	6.282E+02	6.325E+02
	Ave	8.399E+02	8.377E+02	8.331E+02	9.177E+02	8.382E+02	**8.331E+02**	8.411E+02
F4	Std	7.704E+00	7.091E+00	1.009E+01	1.336E+01	8.906E+00	7.130E+00	7.534E+00
	Best	8.286E+02	8.219E+02	8.198E+02	8.923E+02	8.236E+02	8.150E+02	8.246E+02
	Ave	1.278E+03	1.236E+03	1.276E+03	4.095E+03	1.322E+03	**1.228E+03**	1.409E+03
F5	Std	1.271E+02	9.443E+01	1.246E+02	6.937E+02	9.167E+01	9.145E+01	1.545E+02
	Best	1.124E+03	1.043E+03	1.062E+03	2.783E+03	1.092E+03	1.088E+03	1.152E+03
	Ave	2.529E+06	2.563E+05	3.984E+04	7.186E+08	3.568E+05	**3.154E+03**	3.701E+05
F6	Std	7.852E+06	2.797E+05	1.848E+05	4.874E+08	3.539E+05	1.029E+03	4.701E+05
	Best	3.946E+03	2.624E+04	2.197E+03	2.866E+07	4.701E+04	1.857E+03	1.390E+04
	Ave	2.075E+03	2.067E+03	2.062E+03	2.213E+03	2.076E+03	**2.057E+03**	2.084E+03
F7	Std	1.104E+01	1.050E+01	9.056E+00	5.898E+01	1.291E+01	1.092E+01	1.380E+01
	Best	2.056E+03	2.050E+03	2.043E+03	2.086E+03	2.056E+03	2.031E+03	2.059E+03
	Ave	2.255E+03	2.246E+03	2.247E+03	2.491E+03	2.250E+03	**2.243E+03**	2.246E+03
F8	Std	2.987E+01	5.731E+00	9.390E+00	1.233E+02	7.846E+00	8.100E+00	6.978E+00
	Best	2.232E+03	2.233E+03	2.232E+03	2.272E+03	2.236E+03	2.227E+03	2.235E+03
	Ave	2.645E+03	**2.607E+03**	2.636E+03	2.917E+03	2.628E+03	2.623E+03	2.660E+03
F9	Std	3.719E+01	2.268E+01	3.656E+01	1.143E+02	4.151E+01	3.546E+01	4.139E+01
	Best	2.557E+03	2.565E+03	2.555E+03	2.705E+03	2.570E+03	2.569E+03	2.587E+03
	Ave	2.512E+03	2.508E+03	2.506E+03	3.172E+03	2.509E+03	**2.506E+03**	2.514E+03
F10	Std	3.975E+00	2.842E+00	3.063E+00	6.442E+02	3.366E+00	3.036E+00	5.542E+00
	Best	2.508E+03	2.503E+03	2.501E+03	2.539E+03	2.501E+03	2.502E+03	2.507E+03
	Ave	3.035E+03	**2.964E+03**	3.065E+03	4.361E+03	3.107E+03	2.978E+03	3.053E+03
F11	Std	1.888E+02	1.419E+02	1.665E+02	6.562E+02	1.877E+02	1.229E+02	1.354E+02
	Best	2.840E+03	2.786E+03	2.877E+03	3.179E+03	2.879E+03	2.846E+03	2.849E+03
	Ave	2.888E+03	2.876E+03	2.876E+03	3.112E+03	2.875E+03	**2.874E+03**	2.883E+03
F12	Std	1.882E+01	1.113E+01	7.017E+00	9.433E+01	5.619E+00	3.689E+00	1.060E+01
	Best	2.872E+03	2.869E+03	2.871E+03	2.960E+03	2.871E+03	2.871E+03	2.871E+03

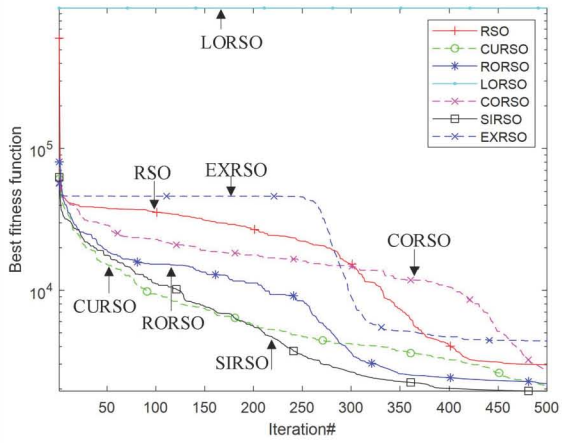

(a) F1

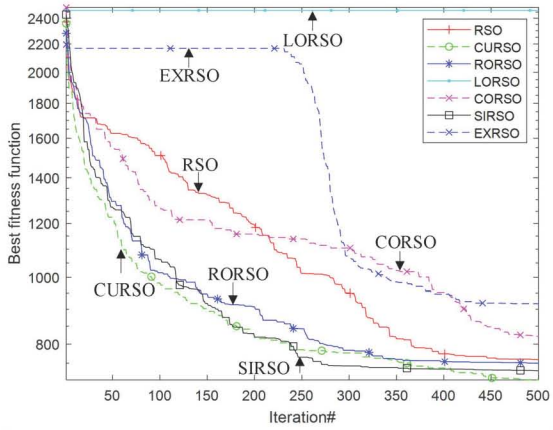

(b) F2

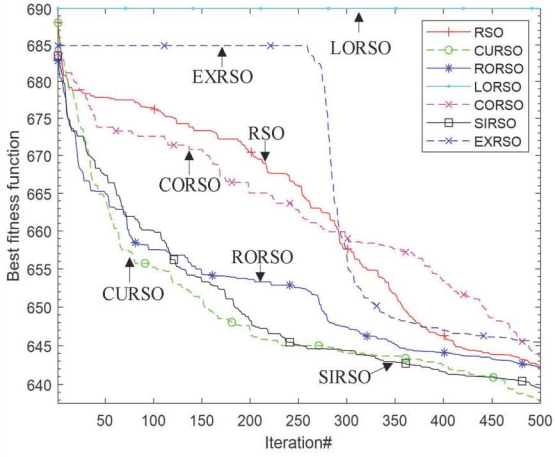

(c) F3

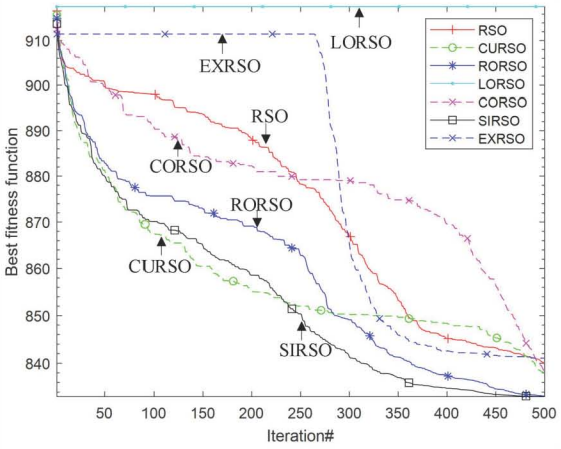

(d) F4

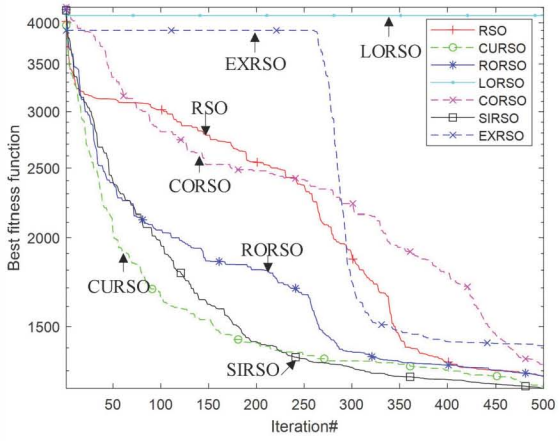

(e) F5

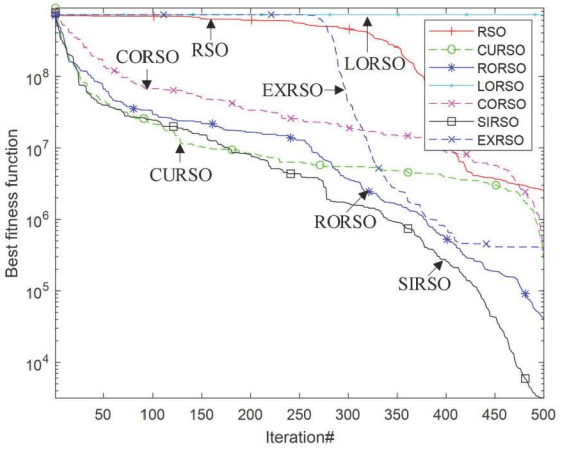

(f) F6

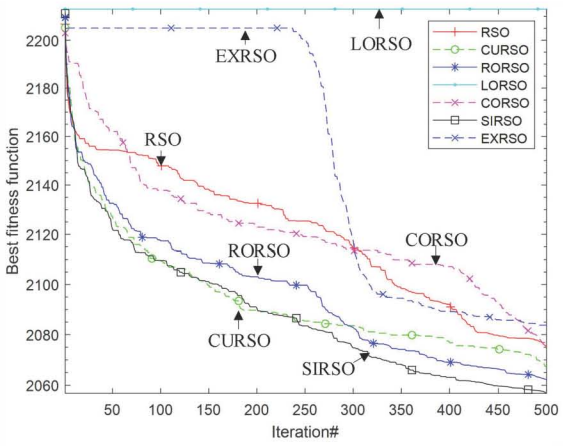

(g) F7

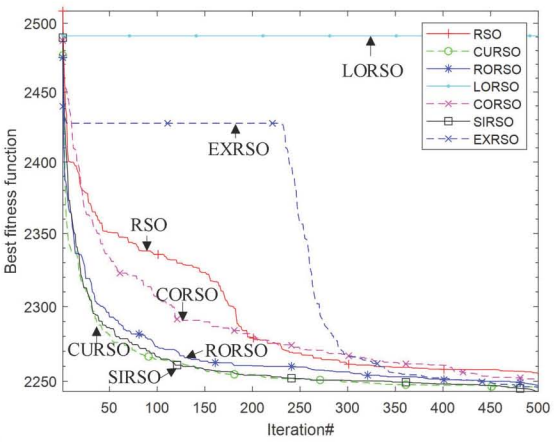

(h) F8

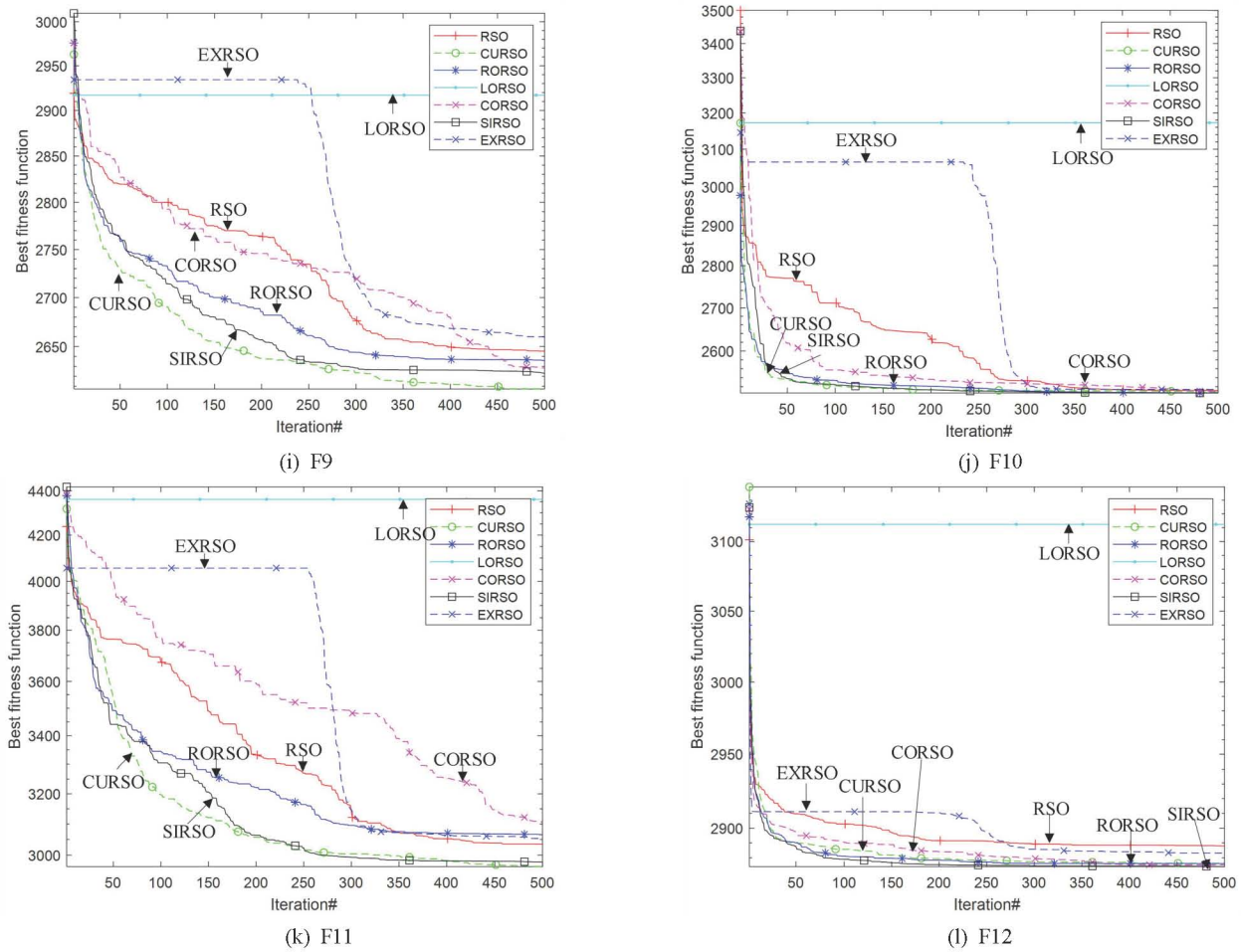

Fig. 3 Simulation results of the test functions.

B. Comparison and Verification Results with Other Algorithms

In this section, we compare the original RSO algorithm with the improved SIRSO algorithm. Additionally, we also compare several other optimization algorithms, including the Waterwheel Plant Algorithm (WWPA), Butterfly Optimization Algorithm (BOA), Frilled Lizard Optimization Algorithm (FLO), Greater Cane Rat Algorithm (GCRA) and Reptile Swarm Optimization Algorithm (RSA). The specific parameter settings for each comparison algorithm are shown in the Table III. The performance of these algorithms is comprehensively evaluated through test functions and compared with existing optimization methods to verify their improvement effects. The population size is set to 50 and the algorithm is iterated 500 times. The average value of 30 runs is taken for plotting.

According to the results in Table IV and Fig. 4, SIRSO achieved the best average values in F1-F12, demonstrating its outstanding stability and optimization capability in handling various optimization problems. Particularly in F1, F6 and F7, SIRSO showed significant advantages, with the smallest average values, standard deviations, and optimal solutions. Additionally, SIRSO also obtained the smallest standard deviations in F2, F3, F8, F10 and F12, indicating its good search stability and consistent performance across multiple experiments. In summary, SIRSO algorithm performed excellently in all test functions, both in terms of optimization accuracy and convergence stability, with strong global search ability and low solution volatility. This makes SIRSO highly potential and valuable in solving various optimization problems, especially in complex optimization problems with high requirements for accuracy and stability.

TABLE III. PARAMETER SETTING OF EACH ALGORITHMS

Number	Algorithm	Parameter settings
1	RSO and its variants	$A \in [0,5)$, $C=[0,2]$, $R \in [1,5]$
2	WWPA	$K=exprnd\ (1,\ 1)$, $r_1=[0,2]$, $r_2=[0,1]$
3	BOA	p=0.8, a=0.1, c=0.01
4	FLO	r is a random number from a normal distribution within the range of 0 to 1, $I=round(1+rand)$
5	GCRA	C is a random number defined within the problem space boundaries, μ=rand[1,4]
6	RSA	A=0.1, B=0.005

TABLE IV. COMPARISON RESULTS WITH OTHER ALGORITHMS

Function	Meteic	RSO	WWPA	BOA	FLO	RSA	GCRA	SIRSO
	Ave	3228.9488	44921.8414	6963.3841	7245.9945	8415.9509	9465.2468	**1968.8903**
F1	Std	1756.4133	87686.3897	1940.7057	1548.1206	2127.4374	2174.8817	**533.9148**
	Best	1557.9856	9624.1047	2980.6138	4500.0913	4557.5700	5009.1846	**1188.3595**
	Ave	796.5924	3361.9089	1750.0389	1068.6251	875.6638	961.9094	**743.7048**
F2	Std	208.5764	1436.5384	588.2695	365.3946	362.9581	279.1190	**119.5784**
	Best	**511.2671**	806.5268	675.7470	523.1106	528.8085	515.5223	583.1947
	Ave	644.5004	687.1367	638.1625	638.8407	647.1069	653.4310	**638.1593**
F3	Std	6.1702	5.9565	5.6264	11.7032	8.0868	6.9270	**5.0189**
	Best	633.3471	667.7987	**625.7305**	616.1449	630.7698	642.5747	628.5298
	Ave	837.4407	887.3353	846.5912	843.5589	849.2253	855.8439	**831.5306**
F4	Std	7.2660	8.5138	6.8588	9.6590	**5.7545**	6.0425	8.2539
	Best	824.3194	867.2299	831.0753	817.8300	837.1843	843.9330	**818.4637**
	Ave	1386.2896	2411.8257	1225.3202	1320.6254	1467.5919	1623.2381	**1200.1160**
F5	Std	143.3328	236.1862	**95.5875**	173.1469	159.3932	229.7205	109.0972
	Best	1104.2295	1864.5037	1015.2704	1050.9925	1086.8594	1243.4166	**1002.6451**
	Ave	2.029E+06	1.767E+08	1.621E+07	1.845E+07	7.135E+07	6.395E+08	**3037.3830**
F6	Std	7.832E+06	7.159E+07	4.955E+07	2.737E+07	4.002E+07	4.758E+08	**1195.9644**
	Best	5.088E+03	4.281E+07	2.670E+05	4.799E+03	1.378E+07	2.226E+07	**1890.9227**
	Ave	2077.8749	2216.2712	2080.2602	2084.0938	2130.6529	2131.6305	**2061.3095**
F7	Std	13.2156	35.0669	13.6042	20.7562	29.1317	35.3784	**9.1741**
	Best	2056.8362	2144.1185	2055.6063	2043.4518	2057.9272	2071.8197	**2040.2820**
	Ave	2256.3530	2391.3455	2272.8076	2245.7037	2248.9105	2259.1620	**2242.1414**
F8	Std	32.0475	88.8684	40.9042	25.1335	7.0573	13.7931	**6.9316**
	Best	2231.7185	2234.7449	2235.8463	**2226.0628**	2234.9996	2241.2769	2229.4853
	Ave	2646.8359	2880.0782	2749.2162	2722.7254	2724.7188	2717.5843	**2624.2573**
F9	Std	39.5516	67.9115	56.3459	**38.2333**	40.1336	40.8137	39.7817
	Best	2571.3104	2771.3402	2640.8231	2658.0873	2646.6880	2619.5469	**2553.7987**
	Ave	2514.8315	3709.6112	2506.6195	2568.0661	2614.7172	2564.6728	**2502.5590**
F10	Std	32.8224	786.4466	2.8604	66.5108	109.3667	40.0952	**0.9060**
	Best	2502.4952	2585.2002	**2501.3786**	2503.6723	2515.6175	2529.5892	2501.5020
	Ave	2975.4502	4797.6816	2962.0833	3238.4568	3220.5219	3382.9827	**2924.7863**
F11	Std	**134.8477**	309.9168	144.6324	376.9186	509.7535	163.3511	149.3450
	Best	2825.8828	3858.6859	2815.0550	2804.5059	2817.3653	3015.2219	**2785.3900**
	Ave	2894.5100	2899.1232	2906.2362	3002.2482	2950.2376	2873.8935	**2873.0500**
F12	Std	28.9892	2.8626	26.5801	54.8452	74.9771	2.6331	**2.1791**
	Best	**2868.8050**	2888.3346	2877.5682	2916.0033	2872.0799	2872.0810	2869.0856

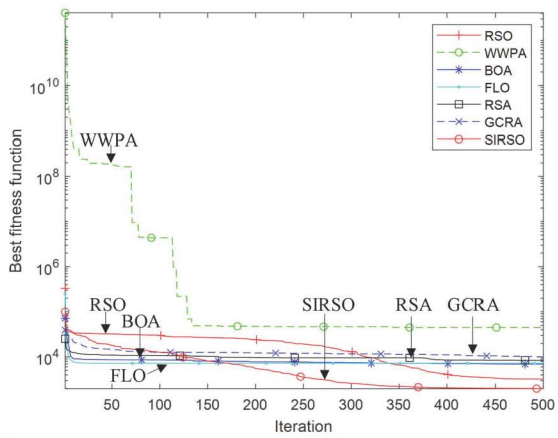

(a) F1

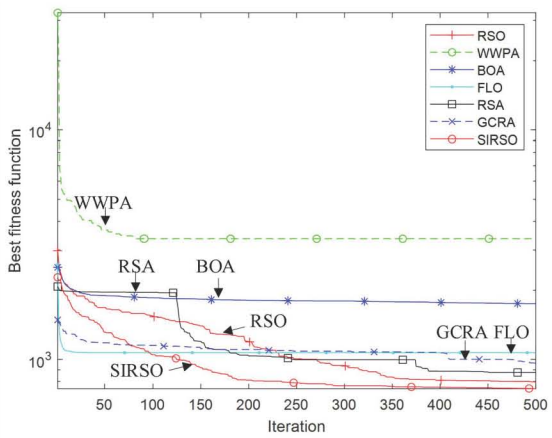

(b) F2

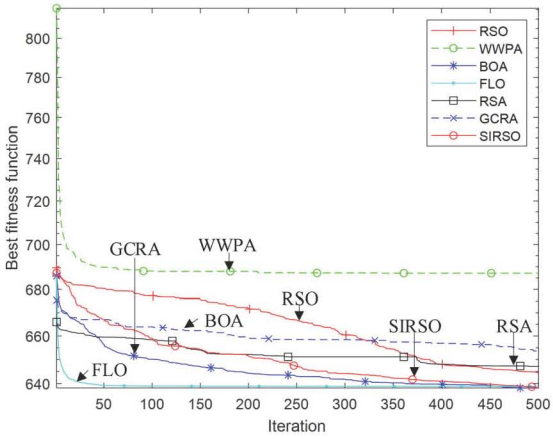

(c) F3

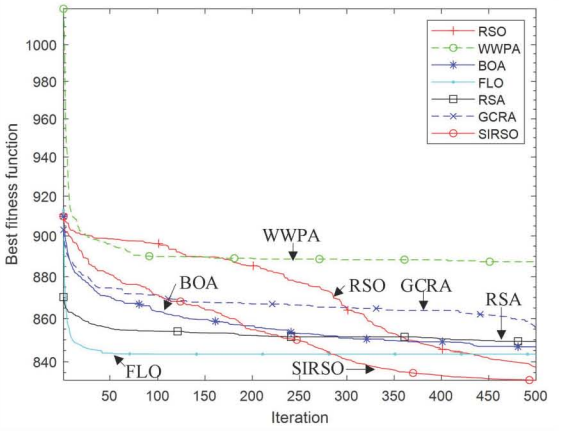

(d) F4

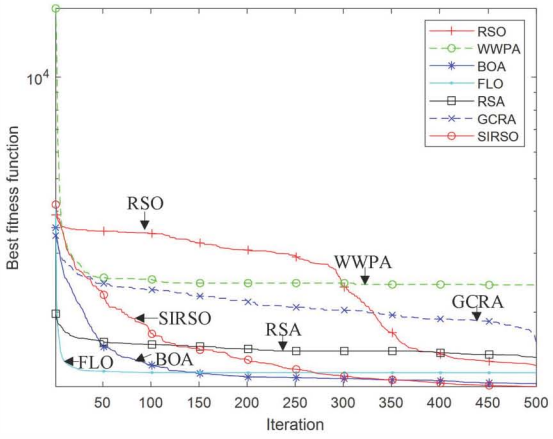

(e) F5

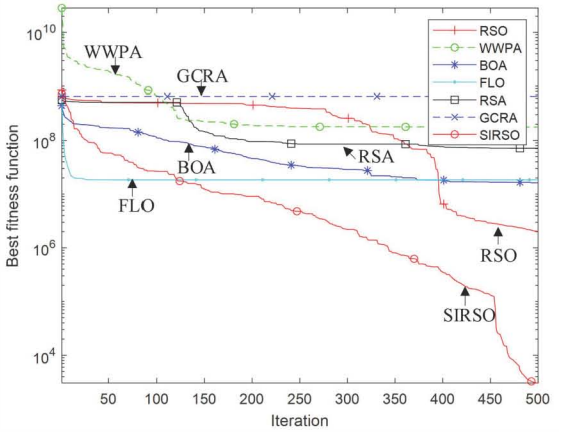

(f) F6

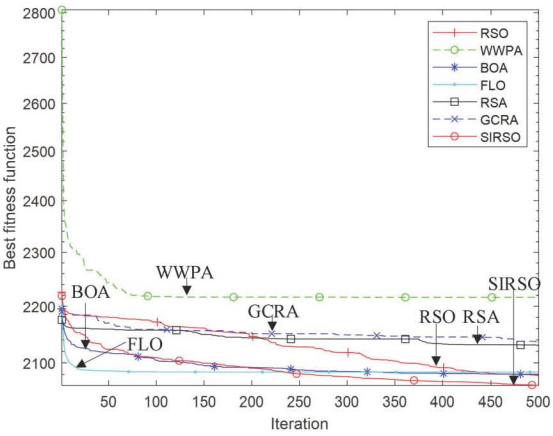

(g) F7

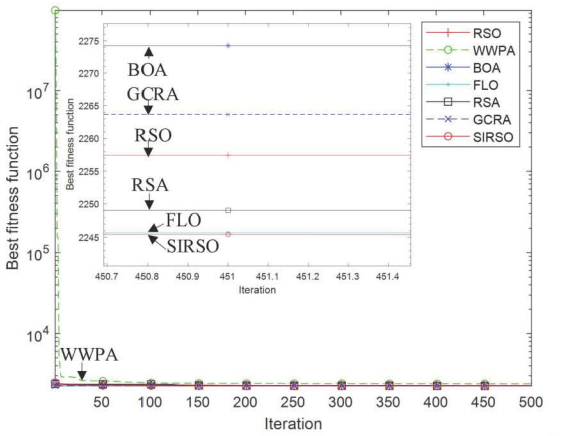

(h) F8

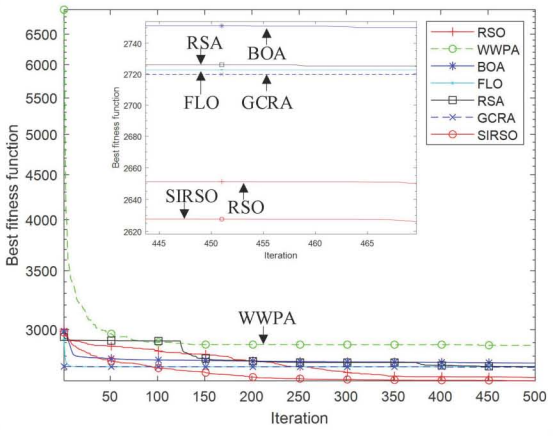

(i) F9

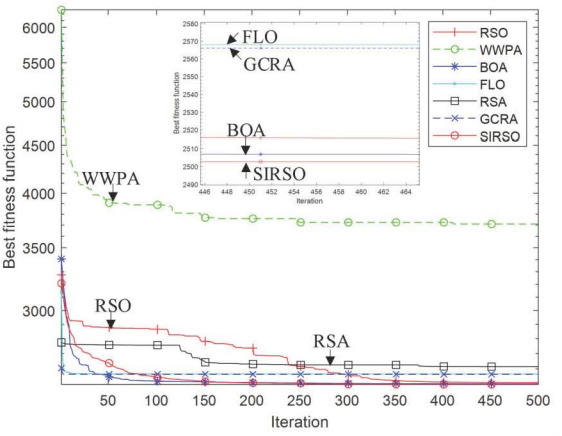

(j) F10

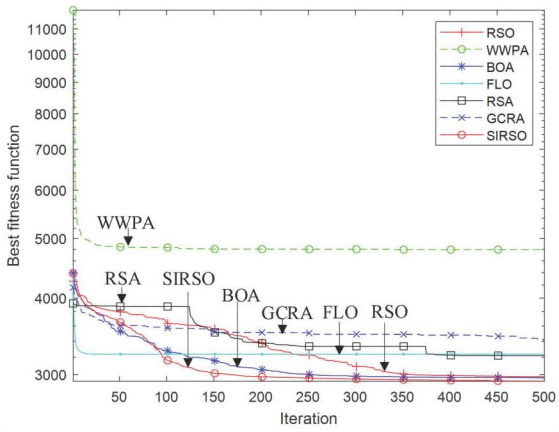

(k) F11

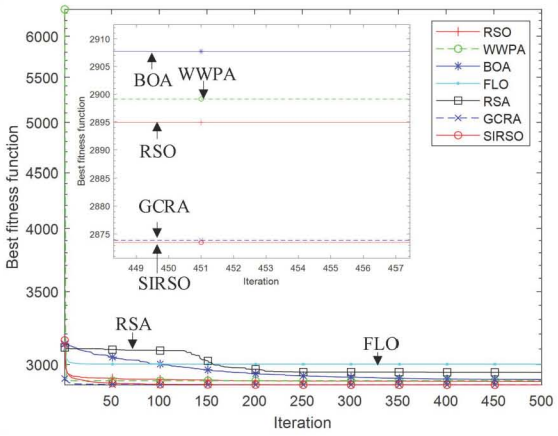

(l) F12

Fig. 4 Simulation results of test functions for each algorithm.

V. Computation Experiments and Result Evaluation of Off-grid Clean Energy Systems

A. Basic Information of System

This paper designs a hybrid renewable energy system, with regional data sourced from the high-cost and low-power demand side scenario proposed in Ref. [20]. The data categories include residential power usage, hourly sunlight during the entire year, ambient temperature, velocity of the wind, and water consumption. The system combines solar energy production, wind turbines, biomass electricity generation, diesel power generation, three kinds of battery packs and bidirectional chargers to supply power to residents and support the operation of reverse osmosis desalination devices.

In the system design [32], the rated power of the biomass generator, converter, diesel generator (DG) and reverse osmosis desalination (ROD) device is set at 5 kW, 55 kW, 50 kW and 2 kWh/m^3 . The optimization objective is the life cycle cost (*LCC*), and the energy cost (*COE*) and diesel consumption are used as environmental indicators. The system reliability is measured by the power supply loss probability (*LPSP*). The life cycle is set at 25 years, and the battery discharge depth is 70%.

Considering the computational complexity, the population size of the optimization algorithm is set at 50, the maximum number of iterations is 100, and every strategy is run ten times, with the mean value used for displaying. The detailed information of the comparison algorithms is presented in Table III. In the Table V, N_{PV}、N_{WT} and N_{BAT} indicate the total amount of photovoltaic modules, turbines for wind power, and battery packs. *TYFCIL*(L) is the annual total fuel consumption, and $TYCO_2$ is the annual carbon dioxide emissions.

The unit of *LCC* is US dollars, and *COE* is expressed as \$/kWh. *LPSP* reflects the proportion of hours with power shortage to the annual load demand hours. During the optimization process, the rated power of the biomass generator, converter, DG and ROD are taken as fixed parameters. The component costs are shown in Table V. The specific models and costs of photovoltaic, wind turbines, batteries and biomass generators are detailed in Ref. [29].

B. Comparison Results of SIRSO with Other Algorithms

It can be seen from Table VI-VIII that the power supply losses of all algorithms are 0, and all can ensure the normal operation of the system. The iterative diagrams of the life cycle costs of the three types of batteries are shown in Fig 5-7. From the perspective of battery types, among the three types of batteries, the system cost is the lowest when nickel-iron batteries are used as energy storage components, with the lowest life cycle cost of 1,015,118 US dollars. Next is lead-acid batteries, with a cost of 1,649,446 US dollars, and lithium batteries have the highest cost, at 2,366,645 US dollars.The cost is strongly related to the battery's service life and replacement frequency.

Although lithium batteries have a high cycle life (3,000 times) and high efficiency (92%), which improves their performance, it further increases their initial manufacturing cost. In contrast, Ni-Fe batteries have the lowest capital cost, thanks to the use of relatively cheap and durable materials. At the same time, their extremely long lifespan (over 30 years and 11,000 cycle life) greatly reduces their life cycle cost, although their efficiency is relatively low (80%) and their daily self-discharge rate is relatively high (1%).

Although lead-acid batteries have the lowest capital cost (410 US dollars), their lifespan is relatively short (3 years or 800 cycle life), requiring frequent replacement. Coupled with their relatively low efficiency (85%), their overall cost is between nickel-iron batteries and lithium batteries. Overall, nickel-iron batteries demonstrate the lowest life cycle cost due to their low capital cost and long lifespan, while lithium batteries, despite their excellent performance, have the highest life cycle cost due to their high capital cost.

Furthermore, there are significant differences among different algorithms in the configuration requirements for photovoltaic panels, wind turbines, and batteries. To further compare the performance of each algorithm in terms of the requirements for system components, this paper ranks the demand quantities of different algorithms on these three independent variables from least to most by using a radar chart shown in Fig. 8-13. The results show that the FLO algorithm has the lowest demand for photovoltaic panels, indicating that it has certain savings in photovoltaic capacity configuration. In terms of the demand for wind turbines and batteries, the improved swarm algorithm SIRSO shows the lowest demand in both aspects,

suggesting that it can effectively reduce the reliance on wind energy and energy storage equipment in multi-energy collaborative optimization and has a higher equipment utilization efficiency. This difference reflects that each algorithm has a certain emphasis on the configuration strategies for different energy equipment in the energy system optimization process, further confirming the differences in adaptability of each algorithm under the optimization goals and constraints.

To ensure the comprehensiveness of the analysis and the intuitive presentation of the results, this study selects two key indicators, namely diesel consumption and life cycle cost, to conduct a systematic comparison of the optimization performance of different algorithms. The ranking results are visually presented through radar charts shown in Fig. 8-13. The main reason for choosing these two indicators is that there is a high positive correlation between diesel consumption and carbon dioxide emissions, while life cycle cost can comprehensively reflect the long-term economic performance of the system, and the trend of energy cost changes is basically consistent with life cycle cost. Therefore, diesel consumption and life cycle cost can be regarded as representative indicators for measuring environmental impact and economic performance.

The experimental results show that there are significant differences in the performance of various algorithms in these two indicators. Among them, the GCRA achieves a better balance between diesel consumption and life cycle cost, without extreme values in any single indicator, demonstrating its ability to coordinate and optimize in terms of economy and environmental sustainability. In contrast, the WWPA has the highest life cycle cost but the lowest diesel consumption, indicating that its optimization strategy is more inclined to reduce fuel consumption, but fails to effectively control the long-term economic expenditure of the system. On the other hand, the improved swarm algorithm SIRSO exhibits opposite characteristics. Although its diesel consumption is the highest, its life cycle cost is significantly lower than that of other algorithms, suggesting that this algorithm has certain advantages in reducing the overall system investment and operation costs, but may come with a higher fuel usage demand. Therefore, in specific applications, the selection of different algorithms should be comprehensively considered in terms of environmental and economic factors to meet the optimization requirements of specific scenarios.

To enhance the algorithm, incorporating a nonlinear decay factor to strengthen the global search capability notably boosts its optimization performance. In lead-acid batteries, the original algorithm cost was \$1,719,948, while the improved algorithm SIRSO cost was \$1,649,446, with a performance improvement of 4.10%. In lithium batteries, the original algorithm cost was \$2,696,973, and the improved algorithm cost was \$2,366,645, with a performance improvement of 12.25%. In Ni-Fe batteries, the original algorithm cost was \$1,190,100, and the improved algorithm cost was \$1,015,118, with a performance improvement of 14.70%. Moreover, from the iteration images, it can be seen that the nonlinear attenuation factor effectively accelerates the optimization speed of the algorithm and achieves a smaller life cycle cost.

Overall, when nickel-iron batteries are used as energy storage components and the SIRSO algorithm is applied, a relatively ideal balance is demonstrated in energy optimization, especially in terms of life cycle cost (LCC) and cost of energy (COE), showing high cost-effectiveness. This makes it appropriate for situations where cost-effectiveness and energy efficiency are crucial

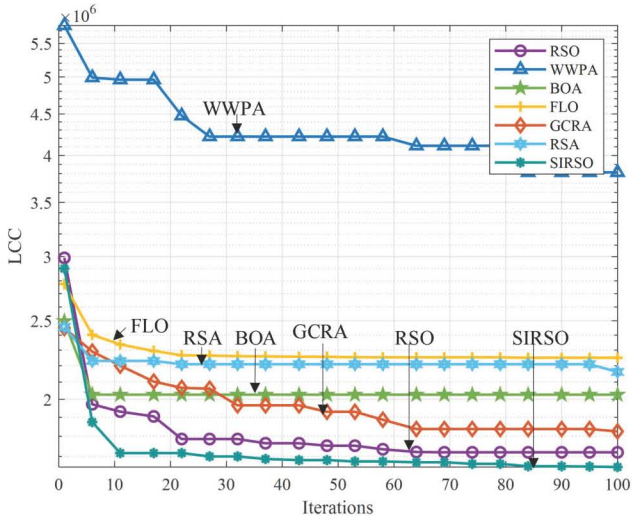

Fig. 5 Comparison chart of LA battery iteration outcomes.

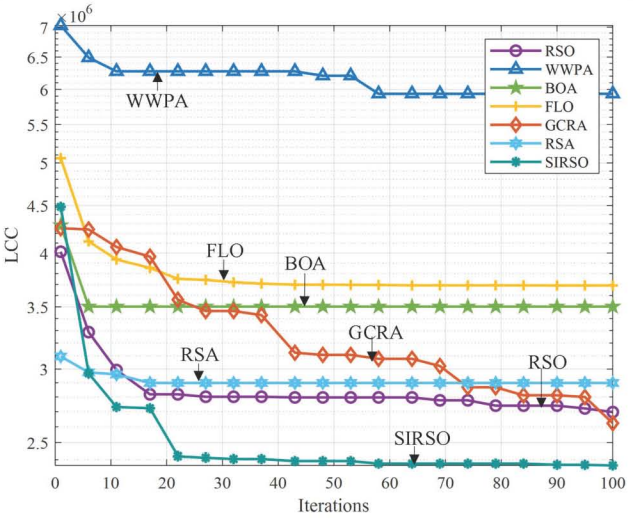

Fig. 6 Comparison chart iteration outcomes for Lithium batteries.

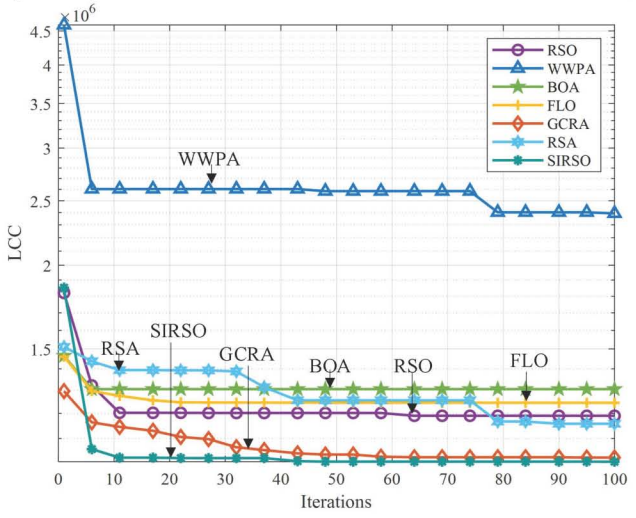

Fig. 7 Comparison chart iteration outcomes for NiFe batteries.

TABLE V. SYSTEM COMPONENT INFORMATION

Parameters	Value	Parameters	Value
Project lifetime	25 years	ROD cap.cost(1m³/day)[[19]]	$532
Nominal interest rate	13%	Initial expense of water tank[19]	256 $/m3
Inflation rate	5%	Initial expense of membrane [19]	0.06 $/m³
Rated power of PV[21]	0.25 kWp	Capital expense of chemicals [19]	0.06 $/m³
Lifetime of PV[21]	25 years	YO&M expense of ROD [19]	0.2 $/m³
Capital expense of PV[21]	$250	No.of MEM Repl./year [19]	2
YO&M cost of PV[21]	$6.25	MEM Replacement cost [19]	0.06 $/m³
Rated power of WT [21]	1 kW	Repl.cost of chemicals [19]	0.06 $/m3
Lifetime of WT [21]	25 years	Rated power of BDC-CAP.C	55 kW
Hub height of WT [21]	20 m	Lifetime of converter [21]	10 years
Cut-in speed of WT [21]	2.5 m/sec	Capital and replacement cost of converter [21]	$5940
Reference height of WT [21]	10 m	YO&M cost of converter [21]	$15
Cut-out velocity of WT [21]	21 m/sec	Efficiency of converter [21]	95%
Rated velocity of WT [21]	11 m/sec	DG(Company:Cummins,Model No:C62.5D5P)[19]	50 kW
Capital expense of WT [21]	$2500	Capital and replacement expense of DG	$5715
YO&M cost of WT [21]	$75	Diesel Price [19]	$0.97
Rated power of BMG [21]	5 kW	YO&M expense of DG	3% of Total annual operative hours of the diesel generator
Life time of BMG [21]	15000 hrs	Quantity of biomass	9 tons/year
Daily operating hoursof BMG	5 hours	Cost of biomass [21]	15 $/ton
BMG CAP.C of 1 kW [21]	$901	Efficiency of BMG [21]	20%
YO&M expense of 1 kW BMG [21]	$27	-	-

TABLE VI. THE OUTCOMES OF SEVERAL ALGORITHMS' OPERATIONS FOR LA BATTERIES

Algorithm	N_{PV} (Number)	N_{WT} (Number)	N_{BAT} (Number)	*TYFCIL* (L)	*TYFCIL Rank*	*TYCO2* (kgs)	*LCC* ($)	*LCC Rank*	*COE* ($/*kWh*)	*LPSP* (%)
RSO	1157	4	288	23745	6	64110	1719948	2	0.3616	0
WWPA	1439	375	519	**3327**	**1**	**8983**	3811813	7	0.8015	0
BOA	1345	69	327	13611	3	36750	2025974	4	0.4260	0
FLO	**986**	128	324	19974	4	53931	2250337	6	0.4732	0
GCRA	1429	7	360	11004	2	29712	1825177	3	0.3838	0
RSA	1055	120	293	20190	5	54514	2161530	5	0.4545	0
SIRSO	1169	**0**	**264**	24178	7	65282	**1649446**	**1**	**0.3468**	0

TABLE VII. THE OUTCOMES OF SEVERAL ALGORITHMS' OPERATIONS FOR LITHIUM-ION BATTERIES

Algorithm	N_{PV} (Number)	N_{WT} (Number)	N_{BAT} (Number)	*TYFCIL* (L)	*TYFCIL Rank*	*TYCO2* (kgs)	*LCC* ($)	*LCC Rank*	*COE* ($/*kWh*)	*LPSP* (%)
RSO	1168	101	240	21489	6	58021	2696973	3	0.5671	0
WWPA	2216	477	493	**2416**	1	**6522**	5935123	7	1.2479	0
BOA	1227	165	363	9869	**2**	26646	3502671	5	0.7365	0
FLO	**945**	171	387	18280	4	49357	3690859	6	0.7761	0
GCRA	1438	**0**	303	17088	3	46136	2623590	2	0.5516	0
RSA	1088	151	246	20145	5	54393	2898927	4	0.6095	0
SIRSO	1273	1	**240**	26761	7	72254	**2366645**	**1**	**0.4976**	0

TABLE VIII. THE OUTCOMES OF SEVERAL ALGORITHMS' OPERATIONS FOR NIFE BATTERIES

Algorithm	N_{PV} (Number)	N_{WT} (Number)	N_{BAT} (Number)	*TYFCIL* (L)	*TYFCIL Rank*	*TYCO2* (kgs)	*LCC* ($)	*LCC Rank*	*COE* ($/kWh)	*LPSP* (%)
RSO	**1176**	29	401	18131	6	48954	1190100	4	0.2502	0
WWPA	2100	158	1313	**1540**	**1**	**4158**	2393049	7	0.5032	0
BOA	1335	60	429	11793	3	31841	1305215	6	0.2744	0
FLO	1228	54	428	12390	4	33454	1244912	5	0.2618	0
GCRA	1503	**0**	490	5573	2	15047	1029697	2	0.2165	0
RSA	1178	20	347	20405	7	55094	1157692	3	0.2434	0
SIRSO	1241	**0**	**343**	15904	5	42940	**1015118**	**1**	**0.2134**	0

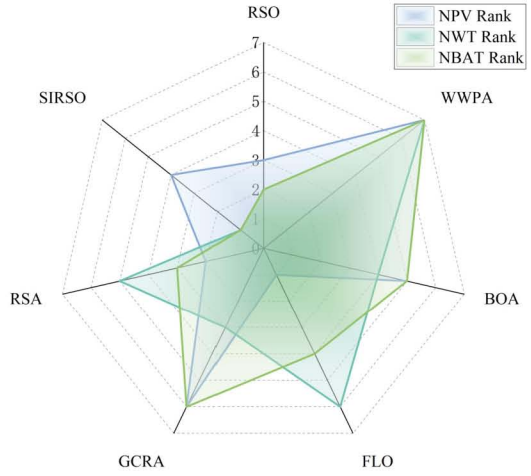

Fig. 8 The N_{PV} rank, N_{WT} Rank and N_{BAT} Rank of LA batteries.

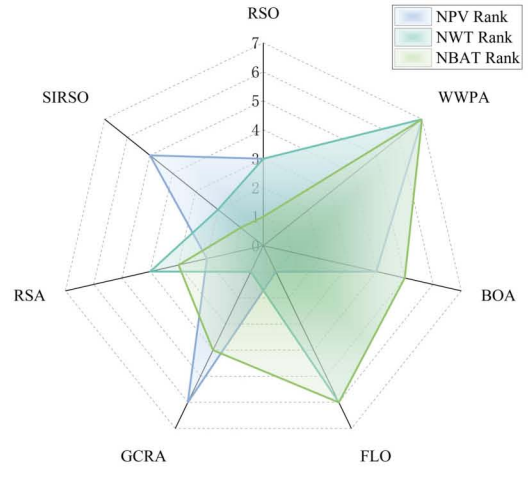

Fig. 9 The N_{PV} rank, N_{WT} Rank and N_{BAT} Rank of Lithium batteries.

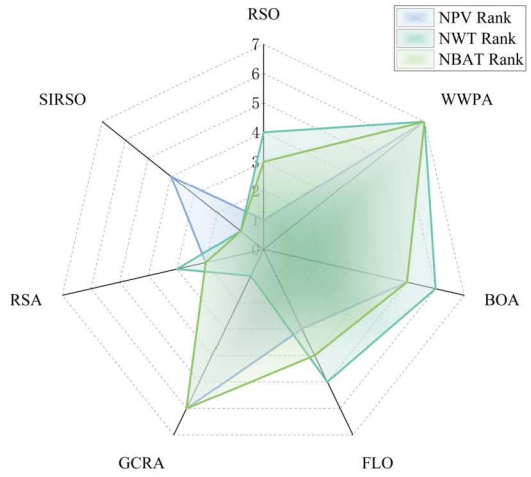

Fig. 10 The N_{PV} rank, N_{WT} Rank and N_{BAT} Rank of NiFe batteries.

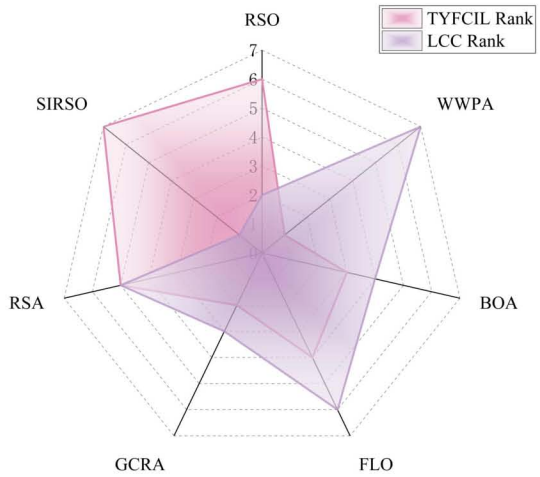

Fig. 11 The TYFCIL Rank and LCC Rank of LA batteries.

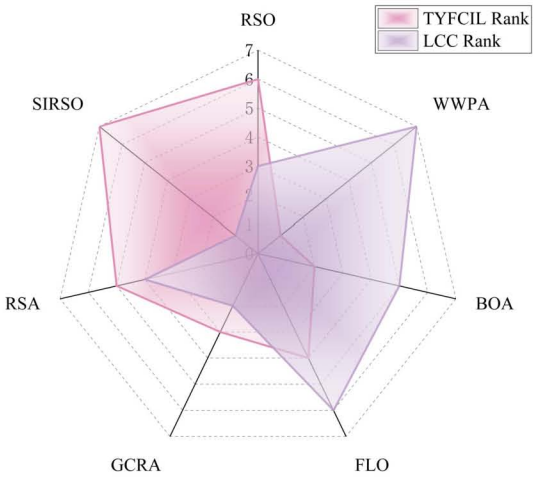

Fig. 12 The TYFCIL Rank and LCC Rank of Lithium batteries.

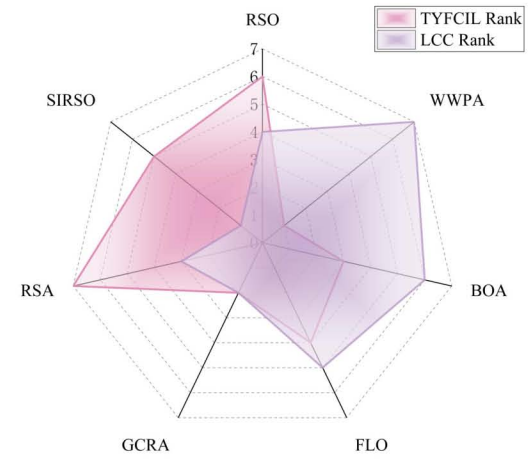

Fig. 13 The TYFCIL Rank and LCC Rank of NiFe batteries.

Overall, when nickel-iron batteries are used as energy storage components and the SIRSO algorithm is applied, a relatively ideal balance is demonstrated in energy optimization, especially in terms of life cycle cost (*LCC*) and cost of energy (*COE*), showing high cost-effectiveness. This makes it appropriate for situations where cost-effectiveness and energy efficiency are crucial.

VI. Conclusion

This paper addresses the issues of slow convergence speed and tendency to get trapped in local optima that exist in the practical application of the rat swarm optimization algorithm. An improved rat swarm optimization algorithm is proposed, which employs six types of decay factors, namely cubic decay factor, cube root decay factor, exponential-binomial distribution decay factor, logarithmic decay factor, sine decay factor, and cosine decay factor, as global search factors to enhance the algorithm's convergence speed and global search capability. The effectiveness of this improvement is verified through the CEC2022 test functions. Lastly, the algorithm is used in a system for clean energy that combines wind turbines, biomass, and solar power generation, diesel generators, reverse osmosis seawater desalination units, battery banks, and rechargeable bidirectional converters. A comparison is made with WWPA, BOA, FLO, GCRA and RSO, and SIIRSO demonstrates superior optimization performance in all cases, confirming the effectiveness of the proposed improvement method.

This study has improved the rat swarm optimization algorithm to address the modeling and optimization issues of microgrid systems. The proposed strategy not only has the potential to enhance the performance of other optimization algorithms but can also be extended to solve optimization problems in other fields. Future research will further expand in the following directions:

1) In terms of battery energy storage technology, future research will consider introducing hydrogen fuel cells. As a storage method with high energy density and environmental friendliness, hydrogen fuel cells are expected to play a significant role in microgrid systems. Therefore, the application of hydrogen fuel cells will be explored in subsequent work to enhance the overall performance and sustainability of the system.

2) Different energy management strategies have an impact on the consumption of different energy sources and life costs. In future research, we will attempt more energy management strategies to jointly plan the modeling problem of microgrids.

References

[1] E. A. Etukudoh, A. Fabuyide, and K. I. Ibekwe, "Electrical engineering in renewable energy systems: a review of design and integration challenges", *Engineering Science & Technology Journal*, vol.5, no. 1, pp. 231-244, 2024.

[2] S. Sinha, and S. S. Chandel, "Review of software tools for hybrid renewable energy systems", *IEEE Transactions on Vehicular Technology*, vol. 32, pp. 192-205, 2014.

[3] A. L. Bukar, and C. W. Tan, "A review on stand-alone photovoltaic-wind energy system with fuel cell: system optimization and energy management strategy", *Journal of Cleaner Production*, vol. 221, pp. 73-88, 2019.

[4] M. Chennaif, M. Maaouane, and H. Zahboune, "Tri-objective techno-economic sizing optimization of off-grid and on-grid renewable energy systems using electric system cascade extended analysis and system advisor model", *Applied Energy*, vol. 305, pp. 117844, 2022.

[5] G. Aniello, H. Shamon, and W. Kuckshinrichs, "Micro-economic assessment of residential PV and battery systems: The underrated role of financial and fiscal aspects", *Applied Energy*, vol. 281, pp. 115667, 2021.

[6] A. Loukatou, P. Johnson, and S. Howell, "Optimal valuation of wind energy projects co-located with battery storage", *Applied Energy*, vol. 283, pp. 116247, 2021.

[7] V. Papadopoulos, J. Knockaert, and C. Develder, "Investigating the need for real time measurements in industrial wind power systems combined with battery storage", *Applied Energy*, vol. 247, pp. 559-571, 2019.

[8] V. Sohoni, S. C. Gupta, and R. K. Nema, "A critical review on wind turbine power curve modelling techniques and their applications in wind based energy systems", *Journal of Energy*, vol. 2016, no. 1, pp. 8519785, 2016.

[9] P. Marocco, D. Ferrero, and A. Ferrero, "The role of hydrogen in the optimal design of off-grid hybrid renewable energy systems", *Journal of Energy Storage*, vol. 46, pp. 103893, 2022.

[10] C. A. Nallolla, and V. Perumal, "Optimal design of a hybrid off-grid renewable energy system using techno-economic and sensitivity analysis for a rural remote location", *Sustainability*, vol. 14, no. 22, pp. 15393, 2022.

[11] I. Viole, G. Valenzuela-Venegas, and M. Zeyringer, "A renewable power system for an off-grid sustainable telescope fueled by solar power, batteries and green hydrogen", *Energy*, vol. 282, pp. 128570, 2023.

[12] T. R. Ayodele, T. C. Mosetlhe, and A. A. Yusuff, "Off-grid hybrid renewable energy system with hydrogen storage for South African rural community health clinic", *International Journal of Hydrogen Energy*, vol. 46, no. 38, pp. 19871-19885, 2021.

[13] V. Arabzadeh, and R. Frank, "Creating a renewable energy-powered energy system: Extreme scenarios and novel solutions for large-scale renewable power integration", *Applied Energy*, vol. 374, pp. 124088, 2024.

[14] G. Sun, Y. Shang, and K. Yuan, "An improved whale optimization algorithm based on nonlinear parameters and feedback mechanism", *International Journal of Computational Intelligence Systems*, vol. 15, no. 1, pp. 38, 2022.

[15] Y. G. Li, M. F. Abdul Ghafir, and L. Wang, "Improved multiple point nonlinear genetic algorithm based performance adaptation using least square method", *Journal of Engineering for Gas Turbines and Power*, vol. 134, no. 3, pp. 031701, 2012.

[16] J. Zhang, and J. Wang, "Improved whale optimization algorithm based on nonlinear adaptive weight and golden sine operator", *IEEE Access*, vol. 8, pp. 77013-77048, 2020.

[17] P. Majumdar, and S. Mitra, "Enhanced honey badger algorithm based on nonlinear adaptive weight and golden sine operator", *Neural Computing and Applications*, vol. 37, pp.367-386, 2024.

[18] M. Zhang, D. Long, and X. Wang, "Improved grey wolf algorithm based on nonlinear control parameter strategy", *2019 Chinese Automation Congres*, pp. 4651-4656, 2019.

[19] P. P. Kumar, and R. P. Saini, "Optimization of an off-grid integrated hybrid renewable energy system with different battery technologies for rural electrification in India", *Journal of Energy Storage*, vol. 32, pp. 101912, 2020.

[20] P. P. Kumar, R. S. Nuvvula, and M. A. Hossain, "Optimal operation of an integrated hybrid renewable energy system with demand-side management in a rural context", *Energies*, vol. 15, no. 14, pp. 5176, 2022.

[21] A. L. Bukar, C. W. Tan, and K. Y. Lau, "Optimal sizing of an autonomous photovoltaic/wind/battery/diesel generator microgrid using grasshopper optimization algorithm", *Solar Energy*, vol. 188, pp. 685-696, 2019.

[22] T. Ma, H. Yang, and L. Lu, "Technical feasibility study on a standalone hybrid solar-wind system with pumped hydro storage for a remote island in Hong Kong", *Renewable Energy*, vol. 69, pp. 7-15, 2014.

[23] A. M. Patel, and S. K. Singal, "Optimal component selection of integrated renewable energy system for power generation in stand-alone applications", *Energy*, vol. 175, pp. 481-504, 2019.

[24] E. M. A. Mokheimer, A. Z. Sahin, and A. Al-Sharafi, "Modeling and optimization of hybrid wind-solar-powered reverse osmosis water desalination system in Saudi Arabia", *Energy Conversion and Management*, vol. 75, pp. 86-97, 2013.

[25] I. D. Spyrou, and J. S. Anagnostopoulos, "Design study of a stand-alone desalination system powered by renewable energy sources and a pumped storage unit", *Desalination*, vol. 257, no. 1-3, pp. 137-149, 2010.

[26] A. Maleki, "Design and optimization of autonomous solar-wind-reverse osmosis desalination systems coupling battery

and hydrogen energy storage by an improved bee algorithm", *Desalination*, vol. 435, pp. 221-234, 2018.

[27] M. Smaoui, A. Abdelkafi, and L. Krichen, "Optimal sizing of stand-alone photovoltaic/wind/hydrogen hybrid system supplying a desalination unit", *Solar Energy*, vol. 120, pp. 263-276, 2015.

[28] A. S. O. Ogunjuyigbe, T. R. Ayodele, and O. A. Akinola, "Optimal allocation and sizing of PV/Wind/Split-diesel/Battery hybrid energy system for minimizing life cycle cost, carbon emission and dump energy of remote residential building", *Applied Energy*, vol. 171, pp. 153-171, 2016.

[29] X. Liu, J. S. Wang, and S. B. Zhang, "Optimization scheduling of off-grid hybrid renewable energy systems based on dung beetle optimizer with convergence factor and mathematical spiral", *Renewable Energy*, vol. 237, pp. 121874, 2024.

[30] S. I. Ao, Smaoui, L. Gelman, and DW. Hukins, "International Association of Engineers", *Design and Off-Design Operation and Performance Analysis of a Gas Turbine*, vol. 2, 2016.

[31] G. Dhiman, M. Garg, and A. Nagar, "A novel algorithm for global optimization: rat swarm optimizer", *Journal of Ambient Intelligence and Humanized Computing*, vol. 12, pp. 8457-8482, 2021.

[32] F. L. Jiang, K. Y. Xue, and Y. N. Wang, "Bi-level Optimal Configuration of Energy Storage System in Distribution Network Using an Improved Grey Wolf Optimization Algorithmr", *IAENG International Journal of Applied Mathematics*, vol. 55, no. 3, pp. 582-593, 2025.